



RESEARCH PAPER

# Hierarchical clustering reveals unique features in the diel dynamics of metabolites in the CAM orchid *Phalaenopsis*

Nathalie Ceusters<sup>1</sup>, Stijn Luca<sup>2</sup>, Regina Feil<sup>3</sup>, Johan E. Claes<sup>4</sup>, John E. Lunn<sup>3, </sup>, Wim Van den Ende<sup>5</sup> and Johan Ceusters<sup>1,6,\*</sup> 

<sup>1</sup> KU Leuven, Department of Biosystems, Division of Crop Biotechnics, Research group for Sustainable Crop Production & Protection, Campus Geel, Kleinhoefstraat 4, 2440 Geel, Belgium

<sup>2</sup> Ghent University, Department of Data Analysis and Mathematical Modelling, Coupure links 653, 9000 Gent, Belgium

<sup>3</sup> Max Planck Institute of Molecular Plant Physiology, Am Mühlenberg 1, 14476 Potsdam-Golm, Germany

<sup>4</sup> KU Leuven, Department of Microbial and Molecular systems, Bioengineering Technology TC, Campus Geel, Kleinhoefstraat 4, 2440 Geel, Belgium

<sup>5</sup> KU Leuven, Department of Biology, Laboratory of Molecular Plant Biology, Kasteelpark Arenberg 31, 3001 Leuven, Belgium

<sup>6</sup> UHasselt, Centre for Environmental Sciences, Environmental Biology, Campus Diepenbeek, Agoralaan Building D, 3590 Diepenbeek, Belgium

\* Correspondence: [johan.ceusters@kuleuven.be](mailto:johan.ceusters@kuleuven.be)

Received 14 November 2018; Editorial decision 1 April 2019; Accepted 1 April 2019

Editor: Christine Raines, University of Essex, UK

## Abstract

**Crassulacean acid metabolism (CAM) is a major adaptation of photosynthesis that involves temporally separated phases of CO<sub>2</sub> fixation and accumulation of organic acids at night, followed by decarboxylation and refixation of CO<sub>2</sub> by the classical C<sub>3</sub> pathway during the day. Transitory reserves such as soluble sugars or starch are degraded at night to provide the phosphoenolpyruvate (PEP) and energy needed for initial carboxylation by PEP carboxylase. The primary photosynthetic pathways in CAM species are well known, but their integration with other pathways of central C metabolism during different phases of the diel light–dark cycle is poorly understood. Gas exchange was measured in leaves of the CAM orchid *Phalaenopsis* ‘Edessa’ and leaves were sampled every 2 h during a complete 12-h light–12-h dark cycle for metabolite analysis. A hierarchical agglomerative clustering approach was employed to explore the diel dynamics and relationships of metabolites in this CAM species, and compare these with those in model C<sub>3</sub> species. High levels of 3-phosphoglycerate (3PGA) in the light activated ADP-glucose pyrophosphorylase, thereby enhancing production of ADP-glucose, the substrate for starch synthesis. Trehalose 6-phosphate (T6P), a sugar signalling metabolite, was also correlated with ADP-glucose, 3PGA and PEP, but not sucrose, over the diel cycle. Whether or not this indicates a different function of T6P in CAM plants is discussed. T6P levels were low at night, suggesting that starch degradation is regulated primarily by circadian clock-dependent mechanisms. During the lag in starch degradation at dusk, carbon and energy could be supplied by rapid consumption of a large pool of aconitate that accumulates in the light. Our study showed similarities in the diel dynamics and relationships between many photosynthetic metabolites in CAM and C<sub>3</sub> plants, but also revealed some major differences reflecting the specialized metabolic fluxes in CAM plants, especially during light–dark transitions and at night.**

**Keywords:** Aconitate, CAM, hexose monophosphates, hierarchical agglomerative clustering, soluble sugars, starch, trehalose 6-phosphate.

## Introduction

Crassulacean acid metabolism (CAM) is a photosynthetic specialization whereby plants optimize water use efficiency by taking up CO<sub>2</sub> predominantly at night when evapotranspiration rates are low. Around 6% of plant species are obligate, facultative or weak CAM plants, and CAM is generally considered a key adaptation for survival in water-limited natural environments. There is also significant interest in introducing CAM into crop species to expand sustainable production of food and biomass on semi-arid, abandoned, or marginal agricultural land (Yang *et al.*, 2015). Traditionally, CAM has been defined within a four-phase framework to describe the various modes of photosynthesis that occur at different times during the day and night (Osmond, 1978): (i) phase I: stomata are open in the dark and external CO<sub>2</sub> is fixed via phosphoenolpyruvate carboxylase (PEPC) into C<sub>4</sub> acids (mostly malate); (ii) phase II: stomata open at the beginning of the light period, and external CO<sub>2</sub> is mainly fixed by ribulose-1,5-bisphosphate carboxylase-oxygenase (Rubisco); (iii) phase III: stomata are closed in the middle of the day, with decarboxylation of malate (catalysed by NAD(P)-malic enzyme (ME) or phosphoenolpyruvate carboxykinase) and refixation of CO<sub>2</sub> by Rubisco; and (iv) phase IV: stomata open towards the end of the day, and external CO<sub>2</sub> is mainly fixed via Rubisco. The C<sub>4</sub> product of night-time carboxylation, malate, is stored overnight in a large central vacuole and subsequently processed the following day when the stomata are closed to release CO<sub>2</sub>, which is then used during C<sub>3</sub> photosynthesis (Borland *et al.*, 2011).

Transitions between light and dark can initiate dramatic reversible changes in metabolism and might serve as environmental cues to acquire the diel CO<sub>2</sub> rhythms (Webb, 2003; McClung, 2006). The temporal separation between the initial carboxylation during the night and subsequent decarboxylation and refixation during the day is necessary to avoid futile cycling of carbon during the diel cycle (Borland and Taybi, 2004; Ceusters *et al.*, 2010). This means that timing is of paramount importance to direct the functioning and interplay between the two carboxylating enzymes. These biological oscillations are orchestrated by interaction between the plant's endogenous circadian clock and the environment. The circadian oscillator operates robustly throughout development and under different environmental conditions (Boxall *et al.*, 2005; Dever *et al.*, 2015). In CAM plants the circadian clock is thought to control PEPC kinase activity (Hartwell *et al.*, 1999). This Ca<sup>2+</sup>-independent, but ATP-dependent, protein kinase brings about reversible phosphorylation of a specific N-terminal regulatory serine residue in PEPC, rendering the enzyme less sensitive to malate inhibition and increasing its activity (Nimmo *et al.*, 1984; Carter *et al.*, 1991; Li and Chollet, 1994). Moreover, PEPC is an allosteric enzyme that is activated by glucose 6-phosphate (Glc6P) and inhibited by L-malate (Carter *et al.*, 1996; Nimmo, 2003). Large differences in sensitivity to malate inhibition have been observed between the dephosphorylated and phosphorylated PEPC, and K<sub>i</sub> (malate) consistently increased during the night (Nimmo *et al.*, 1986; Borland and Griffiths, 1997; Borland *et al.*, 1999; Shaheen *et al.*, 2002). However, in the absence of malate, extracts from *Kalanchoë fedtschenkoi* leaves

harvested in the day or night have essentially the same intrinsic maximum PEPC activity (Nimmo *et al.*, 1986).

To support night-time carboxylation, carbohydrate reserves (starch or soluble sugars) are accumulated in the light period and then remobilized at night to produce phosphoenolpyruvate (PEP), the substrate for PEPC. As such, CAM plants are characterized by a higher nocturnal carbon requirements than C<sub>3</sub> plants in which carbohydrate reserves are degraded to fuel dark respiration. Whilst trehalose 6-phosphate (T6P) fulfils an important function in regulating sucrose and starch metabolism in C<sub>3</sub> plants (Lunn *et al.*, 2014), its potential function in CAM is currently unknown. The synthesis of carbohydrate reserves during the day needs to be coordinated with CO<sub>2</sub> (re)fixation by the Calvin-Benson cycle, and their remobilization at night requires coordination of respiratory pathways (glycolysis, the oxidative pentose phosphate pathway and the tricarboxylic acid (TCA) cycle) with malate production (Ceusters *et al.*, 2014). Various authors have speculated about the significance of changes in cellular metabolite levels in pathways involved in malate and starch synthesis but the precise mechanisms are yet unknown (Sideris *et al.*, 1948; Vickery, 1952; Milburn *et al.*, 1968; Cockburn and McAulay, 1977; Pierre and Queiroz, 1979).

In the presented study, integrated measurements of diel leaf gas exchange, diel metabolite dynamics (e.g. malate, starch, sugars, acids, alcohols, diverse phosphorylated sugars, AMP, ADP, ATP and inorganic phosphate) and PEPC activity were performed in leaves of the CAM orchid *Phalaenopsis* 'Edessa' (moth orchid). However, due to the inherent complexity and shifts in diel metabolism, the statistical processing of large sets of metabolite data from CAM species is challenging and often limited to comparisons of nocturnal/diurnal accumulations/decreases. As such, specific information in the data might be overlooked, especially when integrated with photosynthetic flux and enzyme activity measurements. A hierarchical agglomerative cluster method was applied to extract the maximum information from the data, and the physiological and biochemical relevance of the presented clusters will be discussed, providing further insights into the metabolic regulation of CAM.

## Materials and methods

### *Plant material and sampling*

*Phalaenopsis* 'Edessa' is an obligate CAM plant and belongs to the family Orchidaceae. Vegetative plants were cultivated in a growth room with a constant temperature of 28 °C, a relative humidity of 75% and a 12-h photoperiod (zeitgeber time ZT0–ZT12) with photosynthetic photon flux density (PPFD) of 120 μmol m<sup>-2</sup> s<sup>-1</sup>. Watering was performed twice a week, once with a nutrient solution, Peters 20 N–8.7 P–16.6 K of 1 mS cm<sup>-1</sup>, and once with distilled water. After 6 weeks, leaf samples (*n*=5) were taken from the upper one-third of young fully expanded source leaves during a cycle of 24 h starting from 08.00 h (ZT0) every 2 h until 08.00 h (ZT24) the next morning. Additional samples were taken 5 min before (ZT11.55) and 15 min after (ZT12.15) dusk. The samples from 08.00 h (ZT0 and ZT24) were taken when the lights were turned on whilst the samples taken at 20.00 h (ZT12) were taken in the dark under

a green safety light. Samples were immediately frozen in liquid nitrogen, powdered and stored at  $-80^{\circ}\text{C}$  until analysis.

### Gas exchange measurements

Net  $\text{CO}_2$  exchange was measured on the youngest fully expanded leaves, using a LCi Portable Photosynthesis System (ADC BioScientific Ltd, UK; <https://www.adc.co.uk/>). The top part of the leaf was enclosed in a broad leaf chamber ( $6.25\text{ cm}^2$ ) and the incoming air was passed through a 20-liter bottle to buffer short-term fluctuations in the  $\text{CO}_2$  concentration. Since the LCi system entails an open system configuration, passing fresh air through the system on a continuous basis, environmental conditions as set in the growth room (see plant material and sampling) were tracked. After 6 weeks, gas exchange data were collected over a 24-h period with measurements obtained at 15-min intervals ( $n=3$ ).

### Chemical analyses of metabolites

Soluble sugars (glucose, fructose, sucrose, maltose, and neokestose) were extracted using hot water ( $80^{\circ}\text{C}$ ) and quantified by high performance anion exchange chromatography with pulsed amperometric detection as described by Verspreet *et al.* (2013).

Extraction for measurements of starch,  $\text{P}_i$ , and phosphorylated sugars was performed as described by Chen *et al.* (2002), but with modifications. Approximately 180 mg of powdered tissue was mixed with 450  $\mu\text{l}$  of ice-cold 4% (v/v)  $\text{HClO}_4$ . The mixture was allowed to thaw slowly on ice for 30 min. The resulting suspension was then centrifuged at  $4^{\circ}\text{C}$  for 10 min at 16 200 *g*. The insoluble residue from the perchloric acid extraction was used to determine starch content spectrophotometrically at 340 nm as glucose equivalents (Genesys 10S UV-VIS, Thermo Scientific, USA; <https://www.thermofisher.com>), following digestion with a mix of amyloglucosidase (EC 3.2.1.3) and  $\alpha$ -amylase (EC 3.2.1.1). The analyses were conducted as earlier described by Ceusters *et al.* (2008).  $\text{P}_i$  was measured colorimetrically by mixing a 50  $\mu\text{l}$  aliquot of the soluble  $\text{HClO}_4$  extract with acid-molybdate reagent (prepared by mixing 1 vol. of 0.57 M ascorbic acid with 6 vols of 34 mM ammonium molybdate in 1 N  $\text{H}_2\text{SO}_4$ ). After incubation at  $37^{\circ}\text{C}$  for 1 h, the absorbance at 820 nm was measured in parallel with calibration standards containing 5–80  $\mu\text{M}$   $\text{KH}_2\text{PO}_4$  (Ames, 1966). The remaining supernatant from the  $\text{HClO}_4$  extraction was neutralized at  $4^{\circ}\text{C}$  with 5 M  $\text{K}_2\text{CO}_3$ , and the resulting potassium perchlorate precipitate was removed by 10 min centrifugation at 16 200 *g* and  $4^{\circ}\text{C}$ . Five milligrams activated charcoal was added to the supernatant, and after 15 min at  $4^{\circ}\text{C}$ , removed by 10 min centrifugation at 16 200 *g* and  $4^{\circ}\text{C}$ . The supernatant was used for measurements of different metabolites. Phosphorylated sugars [Glc6P, fructose 6-phosphate (Fru6P) and glucose 1-phosphate (Glc1P)] were measured in a 500  $\mu\text{l}$  reaction mixture containing: 100 mM HEPES–KOH, pH 7.6, 4 mM  $\text{MgCl}_2$ , 0.2 mM NADP, 1 unit glucose 6-phosphate dehydrogenase (G6PDH, EC 1.1.1.49) for Glc6P, then 1 unit glucose phosphate isomerase (EC 5.3.1.9) for Fru6P, and finally 1 unit phosphoglucomutase (EC 5.4.2.2) for Glc1P (Mohanty *et al.*, 1993). Analysis was performed spectrophotometrically by determining the change in absorbance at 340 nm.

Malic acid, pyruvate, 2-oxoglutarate (2-OG), aconitate, shikimate, isocitrate, citrate, succinate, glycerate, glycerol 3-phosphate (Gly3P), 3-phosphoglycerate (3PGA), *myo*-inositol, iso-erythritol, galactinol, ADP-glucose (ADP-Glc), UDP-glucose, trehalose, rhamnose, arabinose, and other phosphorylated sugars, such as mannose 6-phosphate (Man6P), galactose 1-phosphate (Gal1P), T6P, sucrose 6'-phosphate (Suc6P), glucose 1,6-bisphosphate (Glc1,6BP), fructose 1,6-bisphosphate (Fru1,6BP) and PEP were extracted with chloroform–methanol and measured using liquid chromatography coupled to triple quadrupole mass spectrometry (LC/MS–Q3) as described by Lunn *et al.* (2006), with modifications (Figueroa *et al.*, 2016).

The extraction of ATP, ADP, and AMP was based on the method described by Liu *et al.* (2006). About 400 mg of frozen powder was homogenized with ice-cold 4% (v/v)  $\text{HClO}_4$ . The homogenate was left on ice for 1 min and centrifuged for 1 min at 6000 *g* at  $4^{\circ}\text{C}$ . Subsequently the supernatant was neutralized at  $4^{\circ}\text{C}$  with 5 M KOH and left on ice for 30 min to precipitate most of the potassium perchlorate. The supernatant

was used directly for measurement of ATP, ADP, and AMP. ATP was assayed in a 500  $\mu\text{l}$  reaction mixture containing: 100 mM triethanolamine hydrochloride adjusted to pH 7.6 with NaOH, 4 mM  $\text{MgCl}_2$ , 2 mM glucose, 2 mM NADP<sup>+</sup>, 1 unit G6PDH (EC 1.1.1.49) and 0.9 unit hexokinase (EC 2.7.1.1). ATP concentration was determined spectrophotometrically by measuring the change in absorbance at 340 nm upon addition of hexokinase (adapted from Lamprecht and Trautschold, 1974). Both ADP and AMP were measured in a 500  $\mu\text{l}$  reaction mixture containing: 100 mM triethanolamine hydrochloride adjusted to pH 7.6 with NaOH, 1 mM PEP, 33.4 mM  $\text{MgSO}_4$ , 120 mM KCl, 0.33 mM NADH, 12 units lactate dehydrogenase (EC 1.1.1.27) and 9 units pyruvate kinase (EC 2.7.1.40). ADP concentration was determined according to the difference, measured spectrophotometrically at 340 nm, before and after the addition of pyruvate kinase. Subsequently, 8 units myokinase (EC 2.7.4.3) were added to measure AMP spectrophotometrically at 340 nm (Jaworek *et al.*, 1974).

### Enzyme activity of PEPC

The extraction and assay of PEPC were based on the method described by Borland and Griffiths (1997). About 200 mg leaf material was homogenized in 1 ml extraction buffer at  $4^{\circ}\text{C}$  containing: 200 mM Tris–HCl (pH 8.0), 2 mM EDTA, 1 mM dithiothreitol (DTT), 2% (w/v) polyethylene glycol (PEG) 20 000, 1 mM benzamidine and 10 mM malic acid with 240 mM  $\text{NaHCO}_3$ . The homogenate was centrifuged for 2 min at 16 200 *g*. The extract was then desalted by passing twice through a 0.5 ml column of Sephadex G–25, equilibrated with 100 mM Tris–HCl (pH 7.5 at  $4^{\circ}\text{C}$ ), 1 mM DTT, 1 mM benzamidine and 5% (w/v) glycerol. The maximal activity of PEPC was assayed and its  $K_i$  for malic acid estimated using different malic acid concentrations (0.25, 0.5, 2, 8, 16 mM) in a reaction mix (500  $\mu\text{l}$ ) containing: 65 mM Tris–HCl (pH 7.5), 5 mM  $\text{MgCl}_2$ , 0.2 mM NADH, 10 mM  $\text{NaHCO}_3$ , and 2.5 mM PEP. Production of oxaloacetate by PEPC was coupled to oxidation of NADH by the high endogenous NAD-dependent malate dehydrogenase activity in the extracts. The reaction was initiated by the addition of 50  $\mu\text{l}$  of extract and change in absorbance at 340 nm was measured for 4 min at  $25^{\circ}\text{C}$ . Preliminary experiments confirmed a linear decrease of NADH for at least 6 min.

### Data analysis

Clustering was performed using the packages stats, clValid, and mclust from the statistical environment R version 3.5.0 (Brock *et al.* 2008; Scrucca *et al.*, 2016). As the main interest lies in the discovery of curves that are close to each other while clusters are well separated, the Dunn index was used to validate the number of clusters. The Dunn index compares the variance between the members of the clusters with the variance between the means of different clusters. As the diel patterns were equal in size, with measurements every 2 h during a 24-h cycle, a Euclidean distance metric was used as a natural way to express the distance between the diel CAM patterns.

Where appropriate, data were analysed using the statistical software package IBM SPSS Statistics V23. Before carrying out statistical tests, normality of the data was checked by means of the Kolmogorov–Smirnov statistic ( $P>0.05$ ). Throughout the manuscript means are compared by an independent sample *t*-test ( $\alpha=0.05$ ) except for the multiple comparisons by Tukey's Studentized range test ( $\alpha=0.05$ ) in Tables 1–3.

## Results

### Development of a hierarchical clustering method to compare diel CAM patterns statistically

Tissue samples were harvested from young, fully expanded leaves of *Phalaenopsis* 'Edessa' at 2-h intervals throughout a complete 24-h light–dark cycle, with additional sampling around dusk, for metabolite analysis. To process the large

metabolite dataset consisting of about 2500 data points, a hierarchical agglomerative clustering method was applied to group diel patterns with high similarity together. Each pattern consisted of 13 data points with each data point being the mean of five biological replicates. To allow a consistent comparison of patterns ranging from  $\text{nmol g}^{-1}$  FW to  $\text{mmol g}^{-1}$  FW, the data points were first normalized. For each metabolite, general mean and general standard deviation were calculated over the 24-h period of the experiment taking into account all 65 measurements (13 time points  $\times$  5 replicates). Normalization was performed according to the formula  $(x - \text{general mean}) / \text{general standard deviation}$ . Using Euclidian distances, clusters were determined with a complete linkage method and a bottom-up approach, where each observation started in its own cluster and pairs of clusters were merged as one moved up the hierarchy. Based on the Dunn index, seven clusters arose that are displayed in a dendrogram (Fig. 1). We assessed the within-cluster distance (defined as the largest distance between two points within the same cluster) as the number of clusters increased from two to 15 and found that this variance varied in the range 2.40–7.00. Increasing the number of clusters above seven only accounted for a decrease from 3.40 to 2.40 for this variance. Moreover, the between-cluster variability (measured by the square root of the weighted sum of the squared distances between the cluster means and the mean of the whole set of data, the weights being the number of elements in the clusters) varies in the range 7.49–15.05 of which the values in the range 7.49–13.85 are covered by a cluster number up to 7. Additional analyses based on *k*-means and a model-based algorithm confirmed our choice for seven clusters. Clusters showing clear diel trends will be discussed below.

### Clusters of diel metabolite and leaf gas exchange patterns

The first cluster was characterized by daytime degradation and nocturnal build-up (Fig. 2A). For example, malate decreased throughout the day to a minimum level of  $4 \pm 1 \mu\text{mol g}^{-1}$  FW near the end of the light period and then rose during the night to a maximum level of  $61 \pm 4 \mu\text{mol g}^{-1}$  FW before dawn. Similarly 2-OG massively increased from  $15 \pm 4 \text{nmol g}^{-1}$  FW near the end of the light period to  $153 \pm 22 \text{nmol g}^{-1}$  FW before dawn (Fig. 2B). Diel patterns of Glc1,6BP, Fru1,6BP, and Suc6P showed a decline around the middle of the day (ZT6) to minimum levels of  $0.8 \pm 0.3$ ,  $0.3 \pm 0.1$ , and  $0.15 \pm 0.03 \text{nmol g}^{-1}$  FW, respectively. A nocturnal increase was observed, with levels peaking at  $1.4 \pm 0.3$ ,  $1.6 \pm 0.4$ , and  $0.30 \pm 0.05 \text{nmol g}^{-1}$  FW, respectively (Fig. 2C–E).

A second cluster containing T6P, ADP-Glc, 3PGA, and PEP was characterized by an initial accumulation at dawn, followed by a steep decrease during the remainder of the day and rather stable values during the dark period (Fig. 3). T6P showed a gradual, although significant ( $P < 0.05$ ), increase during the first 4 h of the photoperiod followed by a decrease to a relatively stable level of  $1.9 \pm 0.4 \text{nmol g}^{-1}$  FW for the remaining period of the diel cycle (Fig. 3A). ADP-Glc and 3PGA showed a significant ( $P < 0.05$ ) steep increase within the first 2 h of the photoperiod, followed by a gradual decrease ( $P < 0.05$ )

during the remainder of the photoperiod to levels of  $0.7 \pm 0.3$  and  $15 \pm 4 \text{nmol g}^{-1}$  FW, respectively, which remained rather stable during the dark period (Fig. 3B, C). PEP concentrations dramatically increased ( $P < 0.05$ ) at the onset of the day from less than 5 to  $18 \pm 3 \text{nmol g}^{-1}$  FW (Fig. 3D). High PEP levels remained until the middle of the day (ZT6) followed by a gradual decrease to  $2.6 \pm 1.5 \text{nmol g}^{-1}$  FW at dusk. In the dark, PEP remained low and relatively constant at around  $1.3 \pm 0.6 \text{nmol g}^{-1}$  FW.

Figure 1 also illustrates that the organic acids pyruvate, isocitrate, and citrate form a cluster with the sugars trehalose, maltose, neokestose, rhamnose, arabinose, glucose, and fructose. These diel patterns all remained rather stable during the photoperiod and increased slightly near the end of the dark period (Fig. 4). Only pyruvate and trehalose showed a significant nocturnal increase ( $P < 0.05$ ) between ZT12 and ZT23 of  $73 \pm 20$  and  $1.8 \pm 0.7 \text{nmol g}^{-1}$  FW respectively (Fig. 4A, F).

Another cluster comprised succinate and sucrose (Figs 1, 5), and was characterized by a rather stable diurnal phase followed by a significant ( $P < 0.05$ ) nocturnal decrease before rising again in the later part of the night.

As expected, starch (Fig. 6A) showed an inverse diel rhythm compared with malic acid (diel turnover of  $57 \pm 3 \mu\text{mol g}^{-1}$  FW, requiring 171  $\mu\text{mol C}$  atoms of PEP for malic acid synthesis) (Fig. 2A), with starch being the main carbohydrate degraded at night to sustain nocturnal  $\text{CO}_2$  fixation (diel turnover of  $42 \pm 7 \mu\text{mol Glc eq. g}^{-1}$  FW, potentially providing 252  $\mu\text{mol C}$  atoms for PEP synthesis and respiratory production of ATP and NAD(P)H). Additional measurements indicated a lag in starch degradation for at least 1 h (ZT12:  $44 \pm 8 \mu\text{mol g}^{-1}$  FW and ZT13:  $43 \pm 4 \mu\text{mol g}^{-1}$  FW;  $P > 0.05$ ). The pattern of daytime accumulation and night-time degradation was also shared by aconitate and Gly3P (Figs 1, 6). Aconitate showed very low levels during the first half of the photoperiod followed by a steep increase ( $P < 0.05$ ) until a maximum of  $64 \pm 12 \text{nmol g}^{-1}$  FW was reached at dusk (Fig. 6B). Upon darkness aconitate concentrations dramatically decreased ( $P < 0.05$ ) to negligible levels during the rest of the night. Similarly, Gly3P increased during the second half of the photoperiod until a maximum of  $12 \pm 3 \text{nmol g}^{-1}$  FW at dusk, followed by a gradual decrease during the first half of the dark period (Fig. 6C).

*myo*-Inositol, iso-erythritol, galactinol, shikimate, glycerate, and UDPGlc were clustered together, with most of these showing little variation over the diel time course ( $P > 0.05$ ) (Figs 1, 7).

A final cluster was composed of all the measured hexose monophosphates (Glc6P, Fru6P, Glc1P, Man6P and Gal1P) along with the diel leaf gas exchange pattern (Figs 1, 8). After an initial decrease at dawn, all of these metabolites showed an increase during the day followed by a dramatic decrease at the day–night transition (ZT12) halving the pre-dusk concentrations (Fig. 8). By the following sample point (ZT14), the levels of the phosphorylated sugars were already restored to the values seen during the day and remained relatively stable during the dark period but decreased again significantly ( $P < 0.05$ ) at the end of the dark period (ZT22). Based on the clustering approach it can be concluded that the diel dynamics

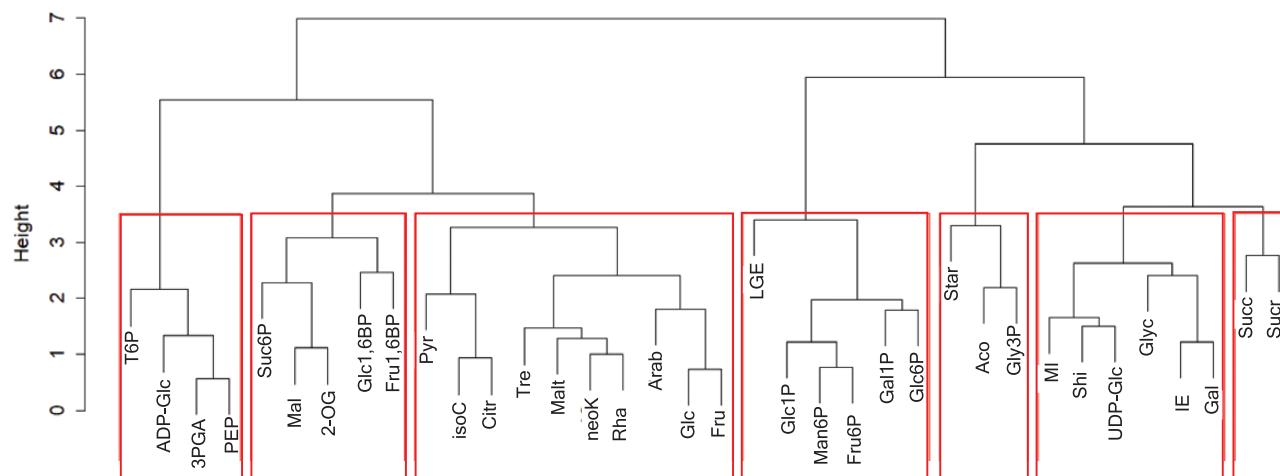


**Fig. 1.** Cluster dendrogram as result of applying a hierarchical agglomerative clustering method to group diel patterns with high similarity together. Based on the Dunn index, seven clusters are formed. 2-OG, 2-oxoglutarate; 3-PGA, 3-phosphoglyceric acid; Aco, aconitate; ADP-Glc, ADP-glucose; Arab, arabinose; Citr, citrate; Fru, fructose; Fru1,6BP, fructose 1,6-bisphosphate; Fru6P, fructose 6-phosphate; Gal, galactinol; Gal1P, galactose 1-phosphate; Glc, glucose; Glc1,6BP, glucose 1,6-bisphosphate; Glc1P, glucose 1-phosphate; Glc6P, glucose 6-phosphate; Gly3P, glycerol 3-phosphate; Glyc, glycerate; IE, iso-erythritol; isoC, isocitrate; LGE, leaf gas exchange; Mal, malic acid; Malt, maltose; Man6P, mannose 6-phosphate; MI, *myo*-inositol; neoK, neokestose; PEP, phosphoenolpyruvate; Pyr, pyruvate; Rha, rhamnose; Shi, shikimate; Star, starch; Suc6P, sucrose 6'-phosphate; Succ, succinate; Sucr, sucrose; T6P, trehalose 6-phosphate; Tre, trehalose; UDP-Glc, UDP-glucose.

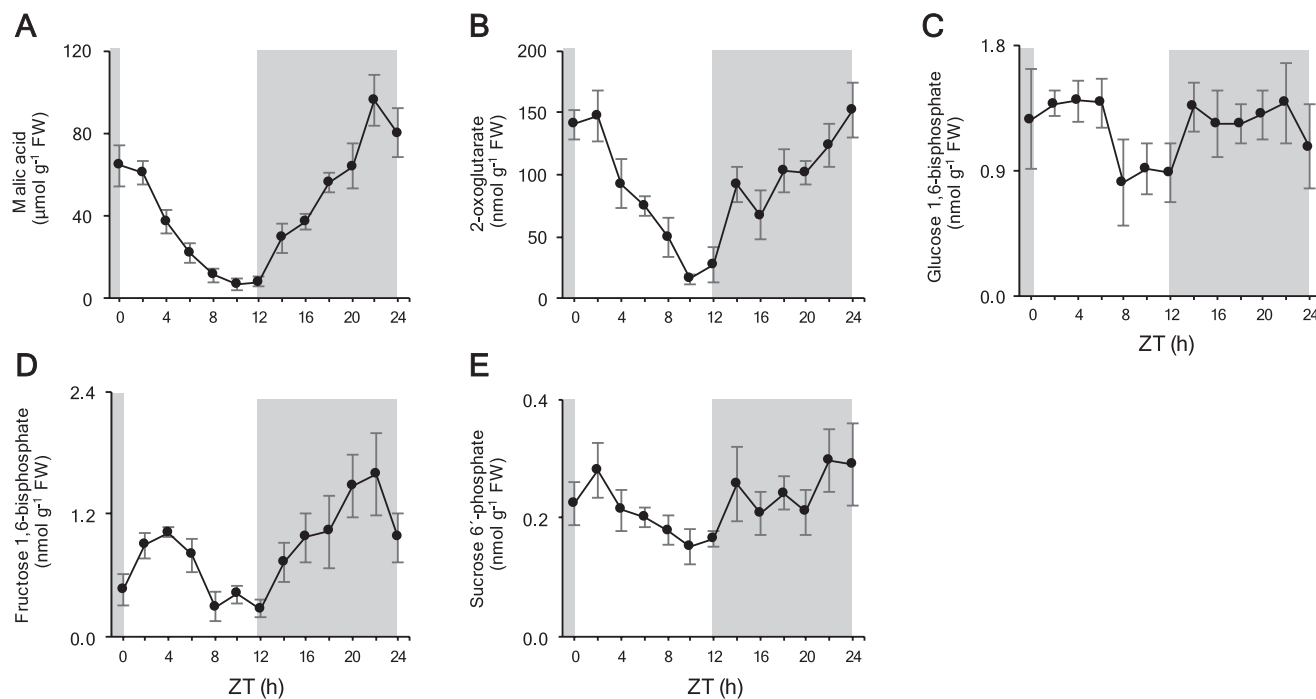


**Fig. 2.** Diel patterns of malic acid (A), 2-oxoglutarate (B), glucose 1,6-bisphosphate (C), fructose 1,6-bisphosphate (D) and sucrose 6'-phosphate (E) for young fully developed leaves of *Phalaenopsis* 'Edessa'. The dark period is indicated in grey. Data are means  $\pm$ SD ( $n=5$ ).

of the hexose monophosphates matched the gas exchange pattern consisting of the four phases of CAM (Fig. 8F).

#### Metabolite changes around the day–night transition

To corroborate and further investigate the marked depression of the hexose monophosphates upon dusk, additional measurements were carried out for Glc6P, Fru6P, and Glc1P at specific time points around the light–dark transition (ZT12) (Table 1).

High concentrations of these metabolites were indeed maintained until the end of the light period (ZT11.55), and when dark set in an immediate decrease was observed (ZT12.15) followed by a gradual recovery (ZT14).

Table 2 shows that the marked depression of hexose monophosphates at dusk was accompanied by a significant increase of 50% for ATP and a significant decrease of 50% for ADP. Measurements at ZT14 confirmed a stable transition towards higher levels of ATP and lower levels of ADP during the night. The pools of both AMP and  $P_i$  remained relatively

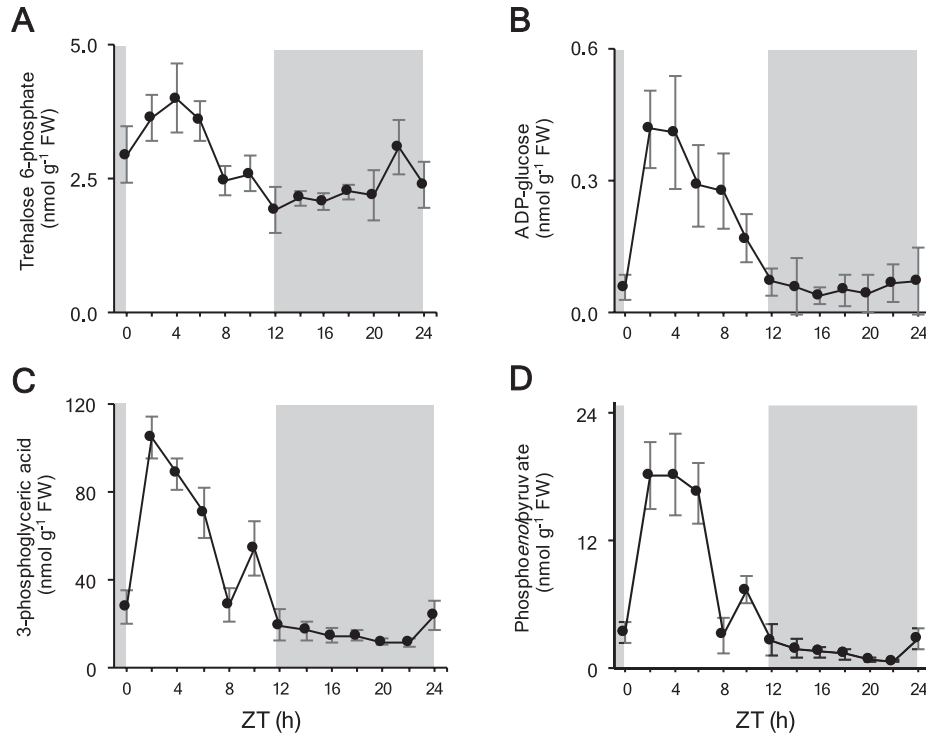


**Fig. 3.** Diel patterns of trehalose 6-phosphate (A), ADP-glucose (B), 3-phosphoglyceric acid (C) and phosphoenolpyruvate (D) for young fully developed leaves of *Phalaenopsis* 'Edessa'. The dark period is indicated in grey. Data are means  $\pm$ SD ( $n=5$ ).

**Table 1.** Contents of phosphorylated monosaccharides in young fully developed leaves of *Phalaenopsis* 'Edessa' at time points close to day–night transition (ZT12)

ZT	Glc6P (nmol g <sup>-1</sup> FW)	Fru6P (nmol g <sup>-1</sup> FW)	Glc1P (nmol g <sup>-1</sup> FW)
11.55	110 $\pm$ 15 <sup>A</sup>	20 $\pm$ 3 <sup>A</sup>	8 $\pm$ 2 <sup>A</sup>
12.15	37 $\pm$ 6 <sup>B</sup>	6 $\pm$ 1 <sup>B</sup>	5 $\pm$ 1 <sup>BC</sup>
14.00	87 $\pm$ 19 <sup>A</sup>	17 $\pm$ 4 <sup>A</sup>	6 $\pm$ 1 <sup>AC</sup>

Data are means  $\pm$ SD ( $n=5$ ) and those in each column followed by a different letter are significantly different by Tukey's Studentized range test ( $P<0.05$ ).

**Table 2.** ATP, ADP, AMP, and P<sub>i</sub> contents in young fully developed leaves of *Phalaenopsis* 'Edessa' at time points close to day–night transition (ZT12)

ZT	ATP (nmol g <sup>-1</sup> FW)	ADP (nmol g <sup>-1</sup> FW)	AMP (nmol g <sup>-1</sup> FW)	P <sub>i</sub> (μmol g <sup>-1</sup> FW)
11.55	20 $\pm$ 3 <sup>A</sup>	22 $\pm$ 4 <sup>A</sup>	3 $\pm$ 2 <sup>A</sup>	1.8 $\pm$ 0.4 <sup>A</sup>
12.15	29 $\pm$ 5 <sup>B</sup>	10 $\pm$ 4 <sup>B</sup>	3 $\pm$ 2 <sup>A</sup>	1.8 $\pm$ 0.3 <sup>A</sup>
14.00	33 $\pm$ 3 <sup>B</sup>	14 $\pm$ 1 <sup>B</sup>	4 $\pm$ 1 <sup>A</sup>	2.1 $\pm$ 0.3 <sup>A</sup>

Data are means  $\pm$ SD ( $n=5$ ) and those in each column followed by a different letter are significantly different by Tukey's Studentized range test ( $P<0.05$ ).

constant without a significant difference between the time points close to the day–night transition.

Measurements of  $K_i$  (malate) for PEPC also revealed significant changes around the light–dark transition (Table 3). At the

**Table 3.** Apparent  $K_i$  of PEPC for malate and maximal activity of PEPC extracted from young fully developed leaves of *Phalaenopsis* 'Edessa' at time points close to day–night transition (ZT12)

ZT	$K_i$ (malate) (mM)	$V_{max}$ (μmol CO <sub>2</sub> g <sup>-1</sup> FW h <sup>-1</sup> )
11.55	6 $\pm$ 1 <sup>A</sup>	79 $\pm$ 6 <sup>A</sup>
12.15	8 $\pm$ 1 <sup>B</sup>	92 $\pm$ 9 <sup>A</sup>
14.00	13 $\pm$ 1 <sup>C</sup>	86 $\pm$ 10 <sup>A</sup>

Data are means  $\pm$ SD ( $n=5$ ) and those in each column followed by a different letter are significantly different by Tukey's Studentized range test ( $P<0.05$ ).

end of the photoperiod (ZT11.55) PEPC was relatively sensitive to malate inhibition, as indicated by a relatively low  $K_i$  value of 6 $\pm$ 1 mM. Within only 15 min of the onset of darkness, PEPC became approximately 50% less sensitive to malate, followed by a further decrease of 50% in malate sensitivity by 2 h later. As expected, no significant differences were observed for the maximal activity of PEPC during the transition between day and night (Table 3).

## Discussion

In CAM plants, strict metabolic control is a prerequisite for C and P homeostasis in order to avoid a range of adverse processes such as futile carbon cycling, depletion of inorganic phosphate, and suppression of photosynthesis (Ceusters *et al.*, 2011, 2013; Borland *et al.*, 2016). It goes without saying that myriad metabolites are involved in these physiological processes. However,

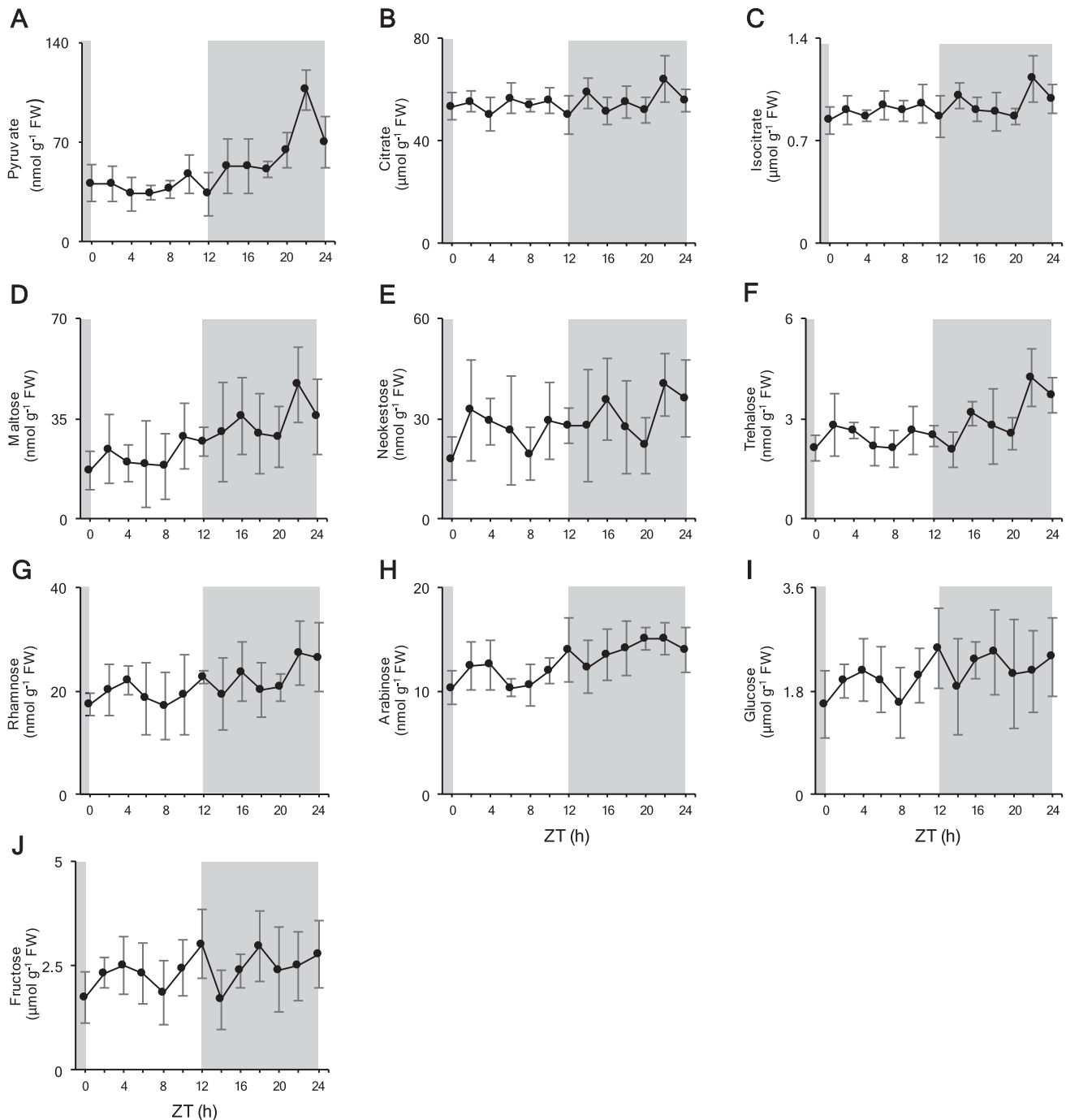


**Fig. 4.** Diel patterns of pyruvate (A), citrate (B), isocitrate (C), maltose (D), neokestose (E), trehalose (F), rhamnose (G), arabinose (H), glucose (I), and fructose (J) for young fully developed leaves of *Phalaenopsis* 'Edessa'. The dark period is indicated in grey. Data are means  $\pm$ SD ( $n=5$ ).

besides a recent study published by [Abraham \*et al.\* \(2016\)](#) focusing on post-transcriptional and post-translational mechanisms governing CAM in *Agave americana* 'Marginata', no extensive diel CAM metabolite datasets have yet been published. Unlike  $C_3$  model plants, such as *Arabidopsis*, important potential signalling molecules such as T6P have not yet been investigated in CAM plants. In addition, large diel metabolite datasets not only offer the opportunity to depict a more comprehensive overview of CAM physiology, but are also essential to parameterize and improve diel flux balance models, allowing powerful computational analyses ([Cheung \*et al.\*, 2014](#); [Shameer](#)

*et al.*, 2018). In this study we used a hierarchical agglomerative cluster method, which can be applied to the diel course data after a simple normalization. Via this novel approach similar metabolite dynamics were grouped together ([Fig. 1](#)), revealing more insights into the metabolic networks involved in CAM. In addition, comparison of the data with published diel data from well-characterized  $C_3$  species revealed both consistencies and marked differences in the relationships between metabolites in CAM and  $C_3$  types of photosynthesis. Being the most comprehensive analysis of diel changes in photosynthetic and central carbon metabolism in a CAM plant to date, this paper

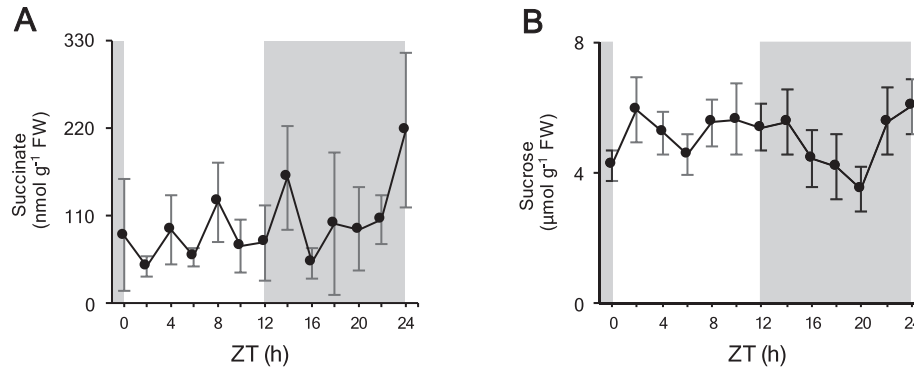


**Fig. 5.** Diel patterns of succinate (A) and sucrose (B) for young fully developed leaves of *Phalaenopsis* 'Edessa'. The dark period is indicated in grey. Data are means  $\pm$ SD ( $n=5$ ).

provides a benchmark for further studies exploring the diversity of metabolism in CAM plants. Specific attention should also be paid to related  $C_3$  and CAM species and facultative or weak CAM species complementing current genomic and transcriptomic work (Brilhaus *et al.*, 2016; Heyduk *et al.*, 2016, 2018).

#### Diurnal metabolite dynamics

At the onset of the day stomata gradually close from phase II towards phase III when decarboxylation of malate provides an internal source of  $CO_2$  to sustain Rubisco fixation. Our results show that the start of phase III was marked by a massive increase (about 400%) in 3PGA, PEP, and ADP-Glc (Fig. 3). High levels of PEP during phase III have earlier been reported in different CAM plants and are mainly attributed to the absence of PEPC activity and the interconversion of pyruvate to PEP in gluconeogenesis (Chen and Nose, 2004). The similar dynamics of 3PGA and ADP-Glc during CAM phase III in our study are consistent with knowledge from  $C_3$  plants, where high levels of 3PGA in the light activate AGPase, thereby enhancing production of ADP-Glc, the substrate for starch synthesis (Tiessen *et al.*, 2002; Mugford *et al.*, 2014). However, the gradual decreases of 3PGA and ADP-Glc over the day in CAM, reflecting the shrinking malic acid store, contrasted with the more abrupt decreases at the end of the day in  $C_3$  plants when dark sets in (Scheible *et al.*, 2000). In accordance with the abundance of triose phosphates during the first 6 h of the day, Fru1,6BP levels rose together with consistent increases in the hexose monophosphate pool (Figs 2, 8). At the end of phase III (ZT8), when malate decarboxylation neared completion, triose phosphates became limiting and Fru1,6BP dropped. At this point the gas exchange curves indicated that the stomata opened (phase IV) and direct Rubisco fixation occurred. With initially rising levels followed by a gradual decrease, T6P showed a similar diel pattern to ADP-Glc and these two metabolites were clustered together (Fig. 3). Under some circumstances, a correlation between T6P and ADP-Glc has also been observed in the  $C_3$  plant *Arabidopsis*. However, it is uncertain whether there is a direct or causal relationship between these two metabolites, because short-term induced changes in T6P levels did not consistently affect either the redox status of AGPase or ADP-Glc levels (Martins *et al.*, 2013,

Figuerola *et al.*, 2016), and the influence of T6P on net starch accumulation during the day has recently been shown to be linked to inhibition of starch degradation in the light, rather than stimulation of ADP-Glc synthesis (Figuerola *et al.*, 2016; Fernandez *et al.*, 2017).

#### Focus on the light–dark transition

The light reactions cease upon the transition from light to dark, making the plant reliant on respiratory pathways for provision of ATP and reducing equivalents to accommodate sucrose synthesis and export. Moreover, in CAM plants, nocturnal carboxylation by PEPC constitutes an important extra energy-consuming process compared with  $C_3$  plants. In the short term, upon onset of the dark, our results indicated a lag in starch degradation of at least 1 h (Fig. 6), which is consistent with some reports from  $C_3$  plants (Pal *et al.*, 2013). At this point the observed drawdown of hexose monophosphates (Fig. 8) can potentially provide reducing power (NADPH) by the action of Glc6P dehydrogenase and 6-phosphogluconate dehydrogenase in the oxidative pentose-phosphate pathway (Dizengremel *et al.*, 2008). Gupta and Anderson (1978) observed no dark inactivation of Glc6P dehydrogenase in the CAM plant *Kalanchoë* 'TetraVulcan'. In CAM plants, an increased nocturnal NADPH pool is beneficial as it provides a source of reducing equivalents for reduction of OAA to malate by NADP-malate dehydrogenase. In addition, the rapid respiration of aconitate stores, which were accumulated in the preceding light period (Fig. 6), via the TCA cycle might contribute to the observed increase in nocturnal ATP levels (Table 2). In *Arabidopsis*, the mitochondrial pyruvate dehydrogenase is known to be activated upon dark, switching the TCA cycle from a dual-linear mode to a cyclic mode, thereby boosting ATP production via oxidative phosphorylation (Sweetlove *et al.*, 2010). Findings that isolated mitochondria from the CAM plant *Kalanchoë daigremontiana* showed considerably increased activity of pyruvate dehydrogenase in phase I compared with phase III support this view (Smith and Bryce, 1992). As such, aconitate might represent an immediately available source of energy upon the light–dark transition to sustain plant metabolism until the main energy supply from starch comes online.

For CAM plants ATP-dependent phosphorylation of PEPC, mediated by PEPC kinase, is essential to lower PEPC's

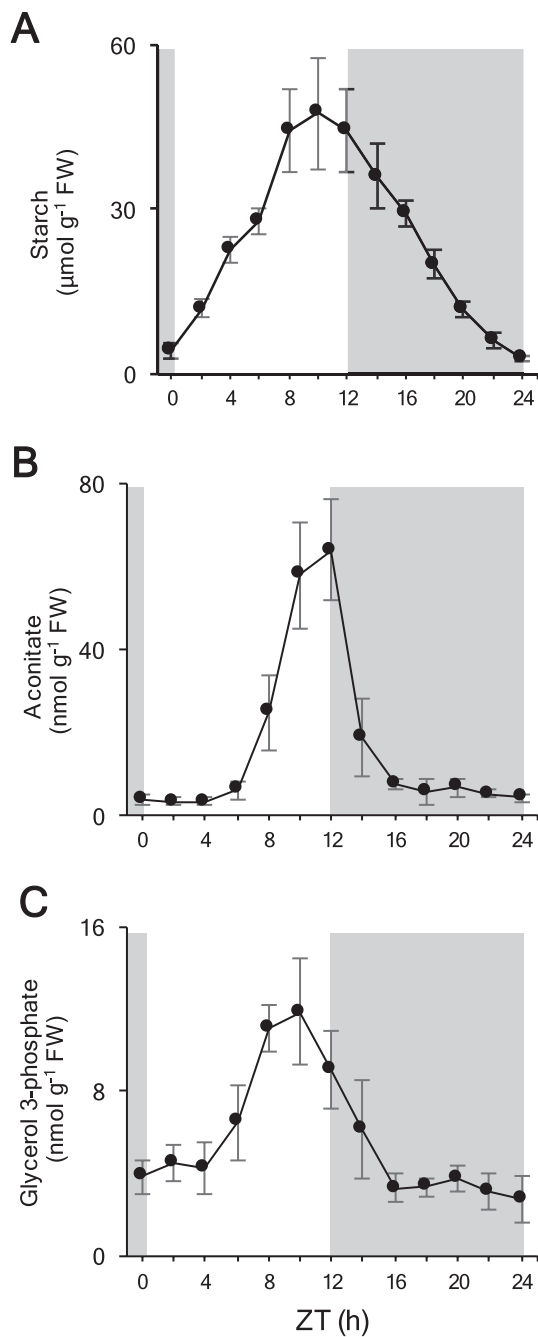


**Fig. 6.** Diel patterns of starch (A), aconitate (B), and glycerol 3-phosphate (C) for young fully developed leaves of *Phalaenopsis* 'Edessa'. The dark period is indicated in grey. Data are means  $\pm$ SD ( $n=5$ ).

sensitivity to malate inhibition (Carter *et al.*, 1991; Li and Chollet, 1994; Izui *et al.*, 2004). The steep  $K_i$  (malate) dynamics (Table 3) show that sensitivity to malate inhibition of PEPC was already seriously diminished from the first hours of the dark period when malic acid levels are still minimal. These results are consistent with the view that PEPC kinase is regulated at the transcriptional level by the circadian clock and high transcript abundance of the kinase has been observed shortly after darkening (Hartwell *et al.*, 1999; Taybi *et al.*, 2000, 2017). Two hours after the onset of darkness, aconitate pools were nearly depleted and significant starch degradation took place. The glucose released by starch degradation will enter glycolysis,

restoring the hexose monophosphates to pre-dusk levels, and is quantitatively sufficient to generate all of the PEP needed for night-time carboxylation by PEPC and accumulation of malate. Indeed there is a surplus of C available from starch degradation. This can be respired via the TCA cycle to provide both ATP and reducing equivalents, which is consistent with the stabilization of the levels of ATP and ADP (Table 2).

#### Nocturnal metabolite dynamics

The nocturnal accumulation of malate and decrease in the light is well known (Winter and Smith, 1996); it is the inverse of the diel pattern observed in  $C_3$  plants and one of the most striking differences between the  $C_3$  and CAM photosynthetic pathways. Interestingly Fru1,6BP, a key intermediate in the Calvin–Benson cycle, gluconeogenesis and glycolysis, clustered together with malate and showed a consistent nocturnal build-up (Fig. 2), which has also been reported earlier in other CAM plants, i.e. *Kalanchoë fedtschenkoi* and pineapple (*Ananas comosus*) (Kenyon *et al.*, 1981; Chen and Nose, 2004). This pattern strongly differs from that in the  $C_3$  plant spinach (*Spinacea oleracea*), which has negligible Fru1,6BP levels in the dark (Gerhardt *et al.*, 1987). As the connection between triose phosphates and the hexose monophosphate pool, Fru1,6BP holds a key position in the biosynthesis and signalling of sucrose (Stitt *et al.*, 1988). In  $C_3$  plants, the forward reaction of FBP aldolase (i.e. aldol cleavage of Fru1,6BP to triose phosphates) is favoured in the dark to feed substrates into the lower half of glycolysis and the TCA cycle. In addition, the *in vivo* activity of sucrose phosphate synthase is low during the night in the  $C_3$  plants spinach and barley (*Hordeum vulgare*), due to post-translational deactivation of the enzyme and low substrate (UDP-glucose and Fru6P) and activator (Glc6P) concentrations in the dark (Stitt *et al.*, 1988; Tetlow and Farrar, 1992).

Our measurements in the CAM plant *Phalaenopsis* 'Edessa' showed that nocturnal carboxylation by PEPC exhausts the PEP pool to negligible levels during the night (Fig. 3). As PEP is considered to exert negative feedback on the Fru6P to Fru1,6BP conversion, the nightly draw-down of PEP allows even higher fluxes through glycolysis and the TCA cycle. This is consistent with the nocturnal increases in respiratory intermediates such as pyruvate, 2-OG and succinate (Figs 2, 4, 5), and is in agreement with the higher nocturnal energetic requirements for CAM plants associated with transport of cytosolic malate into the vacuole across the tonoplast (Winter and Smith, 1996). The nocturnal levels of PEP ( $1.7 \pm 1.0 \text{ nmol g}^{-1}$  FW) were about 40-fold lower than those measured in the  $C_3$  plant *Nicotiana tabacum* (Scheible *et al.*, 2000).

As expected, the nocturnal increase in Fru1,6BP also coincided with rising levels of the hexose monophosphate pool and consequently also Suc6P to pre-dusk levels (Figs 2, 8; Table 1). In  $C_3$  plants, such as Arabidopsis and spinach, a transient decrease of Glc6P, Fru6P, and sucrose has been noticed during the dark period immediately after dusk, followed by partial recovery. For  $C_3$  plants these transient decreases have been attributed to a lag in starch degradation and the accompanying maltose formation (Stitt *et al.*, 1985; Gerhardt *et al.*, 1987; Pal *et al.*, 2013). However, evidence

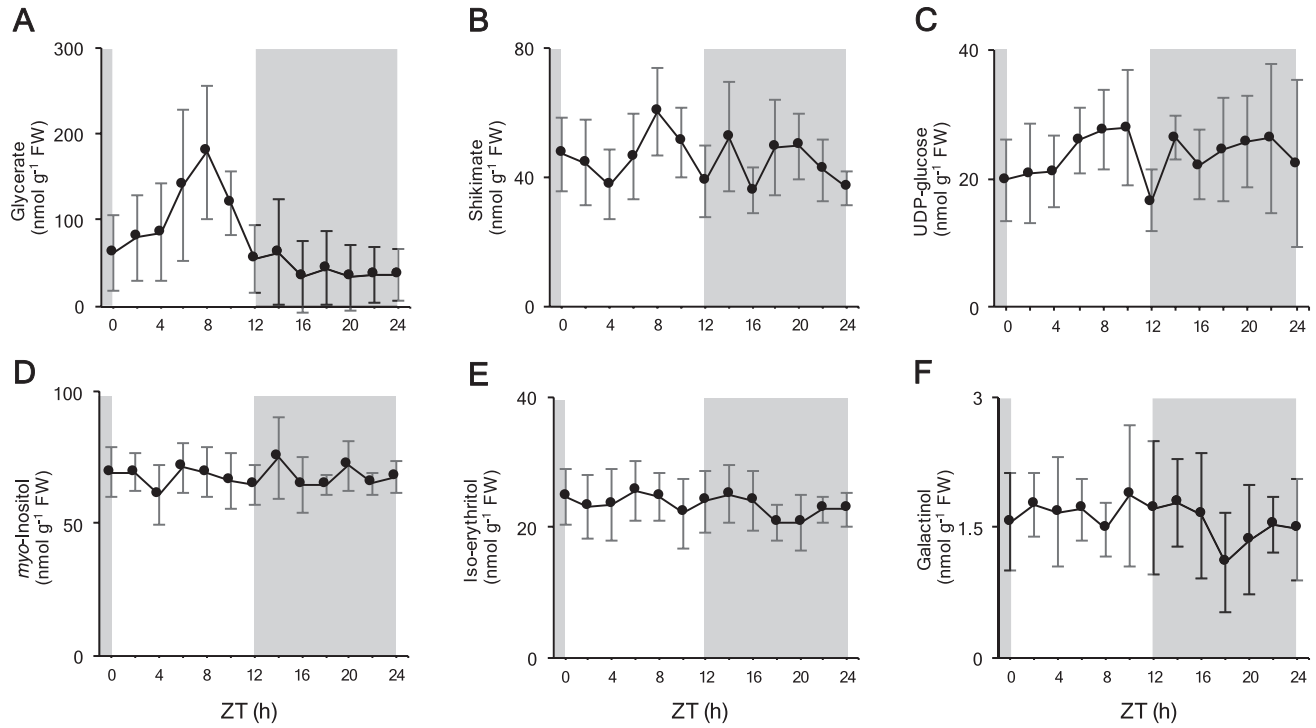


**Fig. 7.** Diel patterns of glycerate (A), shikimate (B), UDP-glucose (C), *myo*-inositol (D), iso-erythritol (E), and galactinol (F) for young fully developed leaves of *Phalaenopsis* ‘Edessa’. The dark period is indicated in grey. Data are means  $\pm$ SD ( $n=5$ ).

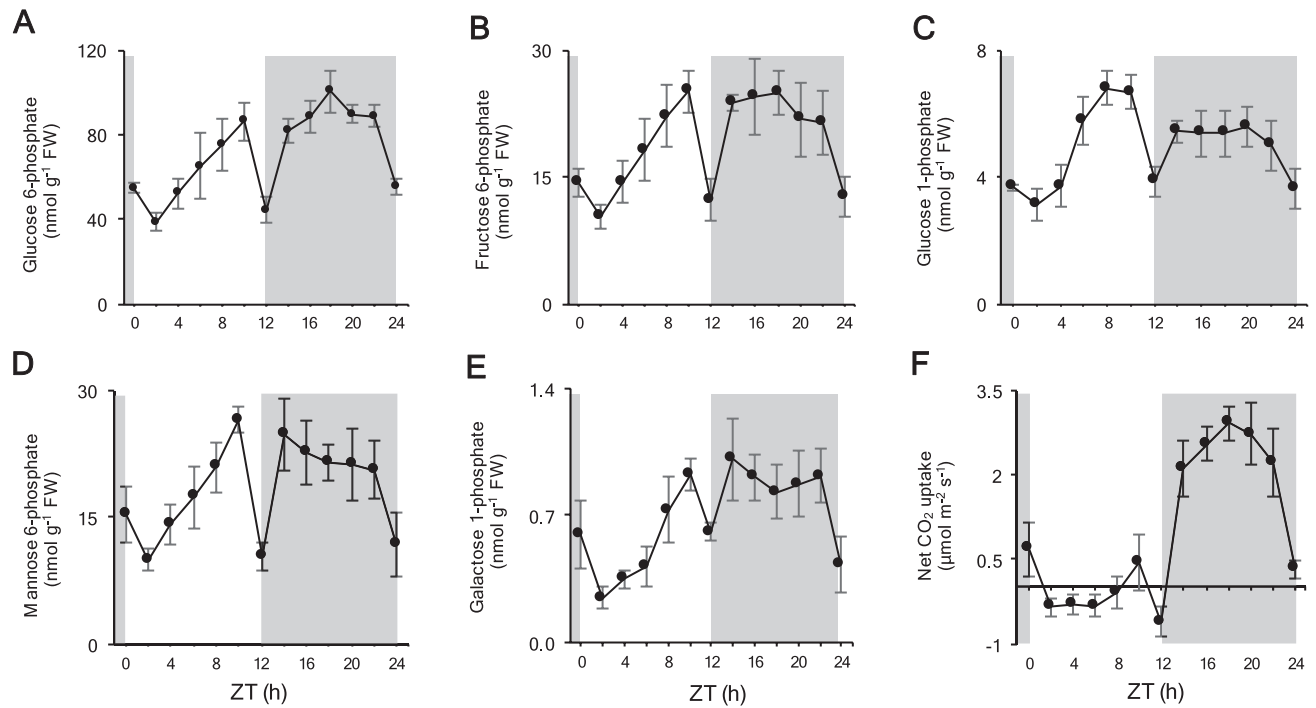


**Fig. 8.** Diel patterns of glucose 6-phosphate (A), fructose 6-phosphate (B), mannose 6-phosphate (C), glucose 1-phosphate (D), galactose 1-phosphate (E), and leaf gas exchange (F) for young fully developed leaves of *Phalaenopsis* ‘Edessa’. The dark period is indicated in grey. Data are means  $\pm$ SD ( $n=5$  for metabolites and  $n=3$  for leaf gas exchange).

is accumulating that the mode of starch degradation is another important point of divergence between CAM and  $C_3$ . In *Arabidopsis*, starch degradation is primarily hydrolytic (producing mainly maltose via  $\beta$ -amylase), but in CAM plants the phosphorylytic route (producing Glc1P via starch

phosphorylase) is thought to dominate (Borland *et al.*, 2016). This view matches with our results for *Phalaenopsis* ‘Edessa’ showing a significant nocturnal increase in Glc6P accompanied by only a small increase in maltose concentrations (Fig. 4) during the dark period.

Low nocturnal levels of T6P (Fig. 3) indicate that this sucrose–signalling metabolite will exert little inhibition on starch degradation during the night (Martins *et al.*, 2013; dos Anjos *et al.*, 2018). In *Arabidopsis* leaves there is a strong positive correlation between T6P and sucrose during the diel cycle (Lunn *et al.*, 2006; Martins *et al.*, 2013; Figueroa *et al.*, 2016), consistent with the postulated function of T6P as a signal and regulator of sucrose levels (Figueroa and Lunn, 2016). In *Phalaenopsis* ‘Edessa’ leaves, T6P was not obviously correlated with sucrose (Figs 3A, 5B). This apparent lack of correlation with sucrose might indicate that T6P has a different function in CAM plants. However, there are other potential explanations for the lack of correlation between T6P and sucrose across the 24-h diel cycle. For example, it is possible that the relationship between T6P and sucrose is shifted as the plant moves between the four distinct metabolic phases during the light–dark cycle, or that storage of sucrose in the large vacuoles of CAM plants masks fluctuations in the more metabolically active pools of sucrose in the cytoplasm that are likely to be the main influence on T6P levels (Martins *et al.*, 2013).

## Conclusion

We proposed a novel approach to compare diel metabolite data that are typical for plants with crassulacean acid metabolism. By applying a hierarchical agglomerative cluster method after normalization, clear trends emerged from grouping diverse diel metabolite patterns from different metabolic pathways such as the Calvin–Benson cycle, glycolysis, oxidative pentose phosphate pathway and the TCA cycle. In line with the higher nocturnal energy requirements for CAM plants, different metabolites such as hexose monophosphates and aconitate were proposed to contribute to energy homeostasis in the CAM plant *Phalaenopsis* ‘Edessa’. Unlike the  $C_3$  model plant *Arabidopsis*, no correlation was found between T6P and sucrose in *Phalaenopsis* ‘Edessa’ leaves. This opens up a question about the function of T6P in CAM plants, and whether it might differ from its function in  $C_3$  plants as a signal and regulator of sucrose levels.

## Acknowledgements

This research was supported by the KU Leuven and by the Max-Planck-Gesellschaft (RF and JEL). Microflor NV is acknowledged for supplying plant material and Kim Vekemans (Geel) and Timmy Reijnders (Leuven) for assistance in the lab.

## References

- Abraham PE, Yin H, Borland AM, *et al.* 2016. Transcript, protein and metabolite temporal dynamics in the CAM plant *Agave*. *Nature Plants* **2**, 16178.
- Ames BN. 1966. Assay of inorganic phosphate, total phosphate and phosphatases. *Methods in Enzymology* **8**, 115–118.
- Borland AM, Barrera Zambrano VA, Ceusters J, Shorrock K. 2011. The photosynthetic plasticity of crassulacean acid metabolism: an evolutionary innovation for sustainable productivity in a changing world. *New Phytologist* **191**, 619–633.
- Borland AM, Griffiths H. 1997. A comparative study on the regulation of  $C_3$  and  $C_4$  carboxylation processes in the constitutive crassulacean acid metabolism (CAM) plant *Kalanchoë daigremontiana* and the  $C_3$ -CAM intermediate *Clusia minor*. *Planta* **201**, 368–378.
- Borland AM, Guo HB, Yang X, Cushman JC. 2016. Orchestration of carbohydrate processing for crassulacean acid metabolism. *Current Opinion in Plant Biology* **31**, 118–124.
- Borland AM, Hartwell J, Jenkins GI, Wilkins MB, Nimmo HG. 1999. Metabolite control overrides circadian regulation of phosphoenolpyruvate carboxylase kinase and  $CO_2$  fixation in Crassulacean acid metabolism. *Plant Physiology* **121**, 889–896.
- Borland AM, Taybi T. 2004. Synchronization of metabolic processes in plants with Crassulacean acid metabolism. *Journal of Experimental Botany* **55**, 1255–1265.
- Boxall SF, Foster JM, Bohnert HJ, Cushman JC, Nimmo HG, Hartwell J. 2005. Conservation and divergence of circadian clock operation in a stress-inducible Crassulacean acid metabolism species reveals clock compensation against stress. *Plant Physiology* **137**, 969–982.
- Brilhaus D, Bräutigam A, Mettler-Altmann T, Winter K, Weber AP. 2016. Reversible Burst of transcriptional changes during induction of Crassulacean acid metabolism in *Talinum triangulare*. *Plant Physiology* **170**, 102–122.
- Brock G, Pihur V, Data S, Datta S. 2008. cValid: An R package for cluster validation. *Journal of Statistical Software* **25**, 1–22.
- Carter PJ, Fewson CA, Nimmo GA, Nimmo HG, Wilkins MB. 1996. Roles of circadian rhythms, light and temperature in the regulation of phosphoenolpyruvate carboxylase in crassulacean acid metabolism. In: Winter K, Smith JAC, eds. *Crassulacean acid metabolism: biochemistry, ecophysiology and evolution*. Heidelberg: Springer, 46–52.
- Carter PJ, Nimmo HG, Fewson CA, Wilkins MB. 1991. Circadian rhythms in the activity of a plant protein kinase. *The EMBO Journal* **10**, 2063–2068.
- Ceusters J, Borland AM, Ceusters N, Verdoodt V, Godts C, De Proft MP. 2010. Seasonal influences on carbohydrate metabolism in the CAM bromeliad *Aechmea* ‘Maya’: consequences for carbohydrate partitioning and growth. *Annals of Botany* **105**, 301–309.
- Ceusters J, Borland AM, Godts C, Londers E, Croonenborghs S, Van Goethem D, De Proft MP. 2011. Crassulacean acid metabolism under severe light limitation: a matter of plasticity in the shadows? *Journal of Experimental Botany* **62**, 283–291.
- Ceusters J, Borland AM, Londers E, Verdoodt V, Godts C, De Proft MP. 2008. Diel shifts in carboxylation pathway and metabolite dynamics in the CAM bromeliad *Aechmea* ‘Maya’ in response to elevated  $CO_2$ . *Annals of Botany* **102**, 389–397.
- Ceusters J, Borland AM, Taybi T, Frans M, Godts C, De Proft MP. 2014. Light quality modulates metabolic synchronization over the diel phases of crassulacean acid metabolism. *Journal of Experimental Botany* **65**, 3705–3714.
- Ceusters J, Godts C, Peshev D, Vergauwen R, Dyubankova N, Lescrinier E, De Proft MP, Van den Ende W. 2013. Sedoheptulose accumulation under  $CO_2$  enrichment in leaves of *Kalanchoë pinnata*: a novel mechanism to enhance C and P homeostasis? *Journal of Experimental Botany* **64**, 1497–1507.
- Chen LS, Lin Q, Nose A. 2002. A comparative study on diurnal changes in metabolite levels in the leaves of three crassulacean acid metabolism (CAM) species, *Ananas comosus*, *Kalanchoë daigremontiana* and *K. pinnata*. *Journal of Experimental Botany* **53**, 341–350.
- Chen LS, Nose A. 2004. Day-night changes of energy-rich compounds in Crassulacean acid metabolism (CAM) species utilizing hexose and starch. *Annals of Botany* **94**, 449–455.
- Cheung CY, Poolman MG, Fell DA, Ratcliffe RG, Sweetlove LJ. 2014. A diel flux balance model captures interactions between light and dark metabolism during day-night cycles in  $C_3$  and Crassulacean acid metabolism leaves. *Plant Physiology* **165**, 917–929.
- Cockburn W, McAulay A. 1977. Changes in metabolite levels in *Kalanchoë daigremontiana* and the regulation of malic acid accumulation in Crassulacean acid metabolism. *Plant Physiology* **59**, 455–458.
- Dever LV, Boxall SF, Kneřová J, Hartwell J. 2015. Transgenic perturbation of the decarboxylation phase of Crassulacean acid metabolism alters physiology and metabolism but has only a small effect on growth. *Plant Physiology* **167**, 44–59.

- Dizengremel P, Le Thiec D, Bagard M, Jolivet Y.** 2008. Ozone risk assessment for plants: central role of metabolism-dependent changes in reducing power. *Environmental Pollution* **156**, 11–15.
- dos Anjos L, Pandey PK, Moraes TA, Feil R, Lunn JE, Stitt M.** 2018. Feedback regulation by trehalose 6-phosphate slows down starch mobilization below the rate that would exhaust starch reserves at dawn in *Arabidopsis* leaves. *Plant Direct*, doi: 10.1002/pld3.78.
- Fernandez O, Ishihara H, George GM, et al.** 2017. Leaf starch turnover occurs in long days and in falling light at the end of the day. *Plant Physiology* **174**, 2199–2212.
- Figuroa CM, Feil R, Ishihara H, et al.** 2016. Trehalose 6-phosphate coordinates organic and amino acid metabolism with carbon availability. *The Plant Journal* **85**, 410–423.
- Figuroa CM, Lunn JE.** 2016. A tale of two sugars: trehalose 6-phosphate and sucrose. *Plant Physiology* **172**, 7–27.
- Gerhardt R, Stitt M, Heldt HW.** 1987. Subcellular metabolite levels in spinach leaves: regulation of sucrose synthesis during diurnal alterations in photosynthetic partitioning. *Plant Physiology* **83**, 399–407.
- Gupta VK, Anderson LE.** 1978. Light modulation of the activity of carbon metabolism enzymes in the crassulacean acid metabolism plant *Kalanchoë*. *Plant Physiology* **61**, 469–471.
- Hartwell J, Gill A, Nimmo GA, Wilkins MB, Jenkins GI, Nimmo HG.** 1999. Phosphoenolpyruvate carboxylase kinase is a novel protein kinase regulated at the level of expression. *The Plant Journal* **20**, 333–342.
- Heyduk K, McKain MR, Lalani F, Leebens-Mack J.** 2016. Evolution of a CAM anatomy predates the origins of Crassulacean acid metabolism in the Agavoideae (Asparagaceae). *Molecular Phylogenetics and Evolution* **105**, 102–113.
- Heyduk K, Ray JN, Ayyampalayam S, Leebens-Mack J.** 2018. Shifts in gene expression profiles are associated with weak and strong Crassulacean acid metabolism. *American Journal of Botany* **105**, 587–601.
- Izui K, Matsumura H, Furumoto T, Kai Y.** 2004. Phosphoenolpyruvate carboxylase: a new era of structural biology. *Annual Review of Plant Biology* **55**, 69–84.
- Jaworek D, Gruber W, Bergmyer HU.** 1974. Adenosine 5-diphosphate and adenosine 5-monophosphate. In: Bergmeyer HU, ed. *Methods of enzymatic analysis*, Vol. 4. Weinheim: Verlag Chemie, 2127–2131.
- Kenyon WH, Holaday AS, Black CC.** 1981. Diurnal changes in metabolite levels and crassulacean acid metabolism in *Kalanchoë daigremontiana* leaves. *Plant Physiology* **68**, 1002–1007.
- Lamprecht W, Trautschold I.** 1974. Determination with hexokinase and glucose-6-phosphate dehydrogenase. In: Bergmeyer HU, ed. *Methods of enzymatic analysis V4*. New York: Elsevier, 2101–2110.
- Li B, Chollet R.** 1994. Salt induction and the partial purification/characterization of phosphoenolpyruvate carboxylase protein-serine kinase from an inducible crassulacean-acid-metabolism (CAM) plant, *Mesembryanthemum crystallinum* L. *Archives of Biochemistry and Biophysics* **314**, 247–254.
- Liu H, Jiang Y, Luo Y, Jiang W.** 2006. A simple and rapid determination of ATP, ADP and AMP concentrations in pericarp tissue of litchi fruit by high performance liquid chromatography. *Food Technology and Biotechnology* **44**, 531–534.
- Lunn JE, Delorge I, Figuroa CM, Van Dijck P, Stitt M.** 2014. Trehalose metabolism in plants. *The Plant Journal* **79**, 544–567.
- Lunn JE, Feil R, Hendriks JH, Gibon Y, Morcuende R, Osuna D, Scheible WR, Carillo P, Hajirezaei MR, Stitt M.** 2006. Sugar-induced increases in trehalose 6-phosphate are correlated with redox activation of ADP-glucose pyrophosphorylase and higher rates of starch synthesis in *Arabidopsis thaliana*. *The Biochemical Journal* **397**, 139–148.
- Martins MC, Hejazi M, Fettke J, et al.** 2013. Feedback inhibition of starch degradation in *Arabidopsis* leaves mediated by trehalose 6-phosphate. *Plant Physiology* **163**, 1142–1163.
- McClung CR.** 2006. Plant circadian rhythms. *The Plant Cell* **18**, 792–803.
- Milburn TR, Pearson DJ, Ndegwe NA.** 1968. Crassulacean acid metabolism under natural tropical conditions. *New Phytologist* **67**, 883–897.
- Mohanty B, Wilson PM, ap Rees T.** 1993. Effects of anoxia on growth and carbohydrate metabolism in suspension cultures of soybean and rice. *Phytochemistry* **34**, 75–82.
- Mugford ST, Fernandez O, Brinton J, et al.** 2014. Regulatory properties of ADP glucose pyrophosphorylase are required for adjustment of leaf starch synthesis in different photoperiods. *Plant Physiology* **166**, 1733–1747.
- Nimmo GA, Nimmo HG, Fewson CA, Wilkins MB.** 1984. Diurnal changes in the properties of phosphoenolpyruvate carboxylase in *Bryophyllum* leaves: a possible covalent modification. *FEBS Letters* **178**, 199–203.
- Nimmo GA, Nimmo HG, Hamilton ID, Fewson CA, Wilkins MB.** 1986. Purification of the phosphorylated night form and dephosphorylated day form of phosphoenolpyruvate carboxylase from *Bryophyllum fedtschenkoi*. *The Biochemical Journal* **239**, 213–220.
- Nimmo HG.** 2003. Control of the phosphorylation of phosphoenolpyruvate carboxylase in higher plants. *Archives of Biochemistry and Biophysics* **414**, 189–196.
- Osmond CB.** 1978. Crassulacean acid metabolism. A curiosity in context. *Annual Review of Plant Physiology and Plant Molecular Biology* **29**, 379–414.
- Pal SK, Liput M, Piques M, et al.** 2013. Diurnal changes of polysome loading track sucrose content in the rosette of wild-type *Arabidopsis* and the starchless *pgm* mutant. *Plant Physiology* **162**, 1246–1265.
- Pierre JN, Queiroz O.** 1979. Regulation of glycolysis and level of the Crassulacean acid metabolism. *Planta* **144**, 143–151.
- Scheible WR, Krapp A, Stitt M.** 2000. Reciprocal diurnal changes of phosphoenolpyruvate carboxylase expression and cytosolic pyruvate kinase, citrate synthase and NADP-isocitrate dehydrogenase expression regulate organic acid metabolism during nitrate assimilation in tobacco leaves. *Plant, Cell and Environment* **23**, 1155–1167.
- Scrucca L, Fop M, Murphy TB, Raftery AE.** 2016. mclust 5: clustering, classification and density estimation using Gaussian finite mixture models. *The R Journal* **8**, 289–317.
- Shaheen A, Nose A, Wasano K.** 2002. *In vivo* properties of phosphoenolpyruvate carboxylase in crassulacean acid metabolism plants: is pineapple CAM not regulated by PEPC phosphorylation? *Environmental Control in Biology* **40**, 343–354.
- Shameer S, Baghalian K, Cheung CYM, Ratcliffe RG, Sweetlove LJ.** 2018. Computational analysis of the productivity potential of CAM. *Nature Plants* **4**, 165–171.
- Sideris CP, Young HY, Chun HH.** 1948. Diurnal changes and growth rates as associated with ascorbic acid, titratable acidity, carbohydrate and nitrogenous fractions in the leaves of *Ananas comosus* (L.) Merr. *Plant Physiology* **23**, 38–69.
- Smith JAC, Bryce JH.** 1992. Metabolite compartmentation and transport in CAM plants. In: Tobin AK, ed. *Plant organelles*. Cambridge: Cambridge University Press, 141–167.
- Stitt M, Wilke I, Feil R, Heldt HW.** 1988. Coarse control of sucrose-phosphate synthase in leaves: Alterations of the kinetic properties in response to the rate of photosynthesis and the accumulation of sucrose. *Planta* **174**, 217–230.
- Stitt M, Wirtz W, Gerhardt R, Heldt HW, Spencer C, Walker D, Foyer C.** 1985. A comparative study of metabolite levels in plant leaf material in the dark. *Planta* **166**, 354–364.
- Sweetlove LJ, Beard KF, Nunes-Nesi A, Fernie AR, Ratcliffe RG.** 2010. Not just a circle: flux modes in the plant TCA cycle. *Trends in Plant Science* **15**, 462–470.
- Taybi T, Cushman JC, Borland AM.** 2017. Leaf carbohydrates influence transcriptional and post-transcriptional regulation of nocturnal carboxylation and starch degradation in the facultative CAM plant, *Mesembryanthemum crystallinum*. *Journal of Plant Physiology* **218**, 144–154.
- Taybi T, Patil S, Chollet R, Cushman JC.** 2000. A minimal serine/threonine protein kinase circadianly regulates phosphoenolpyruvate carboxylase activity in crassulacean acid metabolism-induced leaves of the common ice plant. *Plant Physiology* **123**, 1471–1482.
- Tetlow IJ, Farrar JF.** 1992. Sucrose-metabolizing enzymes from leaves of barley infected with brown rust (*Puccinia hordei* Otth.). *New Phytologist* **120**, 475–480.
- Tiessen A, Hendriks JH, Stitt M, Branscheid A, Gibon Y, Farré EM, Geigenberger P.** 2002. Starch synthesis in potato tubers is regulated by post-translational redox modification of ADP-glucose pyrophosphorylase: a novel regulatory mechanism linking starch synthesis to the sucrose supply. *The Plant Cell* **14**, 2191–2213.
- Verspreet J, Cimini S, Vergauwen R, Dornez E, Locato V, Le Roy K, De Gara L, Van den Ende W, Delcour JA, Courtin CM.** 2013. Fructan

metabolism in developing wheat (*Triticum aestivum* L.) kernels. *Plant & Cell Physiology* **54**, 2047–2057.

**Vickery HB.** 1952. The behavior of isocitric acid in excised leaves of *Bryophyllum calycinum* during culture in alternating light and darkness. *Plant Physiology* **27**, 9–17.

**Webb AAR.** 2003. The physiology of circadian rhythms in plants. *New Phytologist* **160**, 281–303.

**Winter K, Smith JAC.** 1996. Crassulacean acid metabolism: current status and perspectives. In: Winter K, Smith JAC, eds. *Crassulacean acid metabolism: biochemistry, ecophysiology and evolution*. Heidelberg: Springer, 230–246.

**Yang X, Cushman JC, Borland AM, et al.** 2015. A roadmap for research on crassulacean acid metabolism (CAM) to enhance sustainable food and bioenergy production in a hotter, drier world. *New Phytologist* **207**, 491–504.